Study of structural, successional and spatial patterns in tropical rain forests using TROLL, a spatially explicit forest model

Jérôme Chave *

Service de Physique de l'Etat Condensé, DRECAM CEN Saclay, l'Orme des Merisiers, F-91191 Gif sur Yvette, France

Abstract

Competition for light, treefall gap formation and recruitment are the critical phenomena in the genesis of tropical rain forests. These aspects are taken into account to build a new spatially explicit forest growth model called TROLL. Competition for light is modelled by calculating exactly the three-dimensional field of photosynthetically active radiation in the forest understorey. Typically, 10^6 light intensities are computed per hectare at each time step. This light field controls the growth of each tree and establishment/death events. Seed dispersal, dormancy and establishment success as well as a model of treefalls are also included. A special care is paid to the justification and to the validation of each of these modules. The TROLL model is parameterized for a Neotropical rain forest in French Guiana using 12 functional groups of species. Using this model the vertical canopy structure and the tree diametric distribution are investigated. The role of treefalls in maintaining pioneer species is also evidenced. A forest succession scenario is simulated and compared to field data. The model is then used to simulate the recolonization of a previously sterilized area by a rain forest plant community. This scenario is interpreted using information available from palaeorecords over the Holocene period and their validity is discussed. It is suggested that this model could be used to study mosaic-like patterns in rain forests, installation of slowly dispersing species, speciation hypotheses and landscape scale dynamics of rain forests. © 1999 Elsevier Science B.V. All rights reserved.

Keywords: Tropical rain forest; Simulation; Individual-based model; Parallel processing; Canopy gaps; Spatial patterns

1. Introduction

A tropical forest naturally regenerates under several constraints such as light interception (Can-

---

* Present address: Department of Ecology and Evolutionary Biology, Princeton University, Princeton, NJ 08544, USA. Fax: +33-1-6908-8786.

E-mail address: chave@spec.saclay.cea.fr (J. Chave)

ham et al., 1990), treefall gap dynamics (van der Meer et al., 1994) and seed dispersal patterns (van der Pijl, 1982; Ribbens et al., 1994), all of them being crucial for the sylvigenesis (Hallé et al., 1978; Richards, 1996; Whitmore, 1998). A firm understanding of all these processes and of their coupling is a challenge for ecology because tropical ecosystems are currently under threat of

strong anthropogenic disturbances. This rapid deforestation could in turn have a strong influence on the global climate of the next century (Phillips et al., 1998). A related issue is to understand how tropical trees communities can have recolonized large areas after the end of the last glacial stage (Servant et al., 1993; Bush, 1994; Schwartz et al., 1996; Charles-Dominique et al., 1998) in order to better predict how rain forests could recover if conservation policies were adopted. Such issues can be addressed through modelling techniques as it is shown in the present article.

It has long been recognized that the most crucial step in the sylvigenetic cycle is the formation of natural canopy openings. This observation has motivated the 'gap model' approach (Botkin et al., 1972; Shugart, 1984; Prentice and Leemans, 1990; Schenk, 1996) where forest patches of size 0.1–0.4 ha, (or eco-unit, after Oldeman, 1990) have their own dynamics. KIAMBARAM (Shugart et al., 1980; Shugart, 1984) and FORMOSAIC (Liu and Ashton, 1998) are two examples of gap models applied to rain forests. The gap model approach turns out to give reliable results for assessing short term scenarios. Nevertheless several problems result from this approach.

Firstly, it often avoids the mechanistic modelling of tree interactions by incorporating complicated descriptions of tree growth with interaction indexes (however, see Köhler and Huth, 1998). The gap size is fixed and therefore small-scale light fluctuations (sun flecks) cannot be modelled, although they are of crucial importance in dense forest understoreys. Moreover treefalls are not modelled mechanistically but patches are usually cleared randomly. Secondly, seed dispersal is generally modelled only by assuming that seeds are always present. Recent field work has shown that seed dispersal limitation is crucial for maintaining species diversity (Hubbell et al., 1999) thus confirming the winning-by-forfeit scenario (Hurtt and Pacala, 1995). Thirdly, spatial effects are difficult to reproduce since neighbouring patches are not interacting in most gap models. Bossel and Krieger (1994) and Lischke et al. (1996) have attempted to resolve this difficulty by introducing nearest neighbour

patches interactions. A direct consequence of this lack of spatialization is that gap models must resort to a sampling over several simulations (Monte-Carlo average) to get statistically significant results. In the presence of spatial correlations, averaging over a statistical sample of independent plots smaller than the correlation length of the system under study is not equivalent to taking one large plot. Here, seed dispersal limitation implies a correlation length greater than 100 m. The two-dimensional model of canopy crown due to Moravie et al. (1997) should be mentioned as an interesting direction to overcome this problem.

Due to the increasing power of computers it is now possible to model directly the trees and their interactions, avoiding aggregation procedures. A good example of this approach is the SORTIE model (Pacala et al., 1996; Deutschman et al., 1997) in which many important aspects of dynamic processes in a temperate forest are individually modelled and precisely parameterized (growth, mortality, dissemination). Nonetheless SORTIE requires a large number of data to be fully parameterized and, except for a few well documented plots such as Barro Colorado Island (Panama), Mudumalai (India) or Pasoh (Malaysia), this program is difficult to apply in rain forests. As Vanclay (1995) remarks, 'The challenge is to provide sufficient physiological and ecological basis to ensure realistic predictions under a variety of sites and stand conditions, even when empirical data for calibration are limited'. Hence we are in the need of simple, mechanistic-based approaches for tropical forests. Moreover existing models cannot account for large-scale spatial patterns such as the migrations of plant communities observed in palaeorecords since the last glacial maximum.

In the present work we describe and we use TROLL, a new succession model which attempts to overcome both difficulties. The sub-models of competition for light, dispersion and treefall gaps are all built on simple mechanistic and physiologic hypotheses (Section 2). The number of parameters is reduced as much as possible to make the parameterization easier (Section 3). Thanks to a powerful parallel computer, large

forest stands are simulated and the Monte-Carlo sampling is avoided. TROLL is shown to reproduce structural (diametric distributions) and successional patterns of a tropical rain forest with a good agreement. In addition a rain forest invasion is simulated and it is compared to available information of the forest migrations in the Holocene period. Discussions and perspectives are gathered in Section 5.

2. Description of the model

TROLL simulates the growth of trees located on a study plot of variable size. In one time step a discrete three-dimensional field (voxel field) of leaf density is computed, trees are grown or killed in function of the local light availability (or by treefalls), and the seed bank is updated by the dispersion of seeds produced by fruiting trees. The dynamics is discrete in time and the time step is fixed to 1 year. This choice is easily generalized to shorter time steps which should be taken when modelling seasonal effects such as rainfall fluctuations. In the present work, we assume a constant climate (temperature, rainfall, duration of the dry

period), therefore a time discretisation into steps of 1 year provides a detailed enough description of the dynamics.

Only woody plants of more than 1 cm diameter at breast height (dbh) are considered. Due to space exclusion of stems and root systems, a minimal surface is necessary for a tree to survive. This fixes a minimal nearest neighbour distance which is called λ. In this study the value $\lambda = 1$ m was taken. The maximal stem number is therefore 10 000 stems per hectare, which is roughly twice more than those counted in field studies (Hubbell and Foster, 1990; Condit, 1995b). The study area is discretised into squares of edge λ in which only one tree can grow. This assumption saves computer memory and avoids population blow-ups.

2.1. Tree description

One tree is spatially defined by several geometric variables: dbh, D, height H, crown radius R and crown depth h (Fig. 1). The age A is recorded for each tree, as well as a species label. In the present version, a set of parameters is defined for each species (see section parameterization and Table 1).
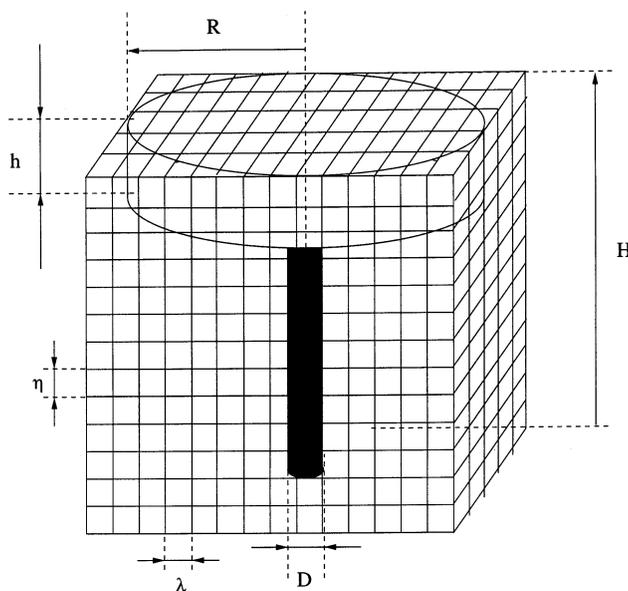

Fig. 1. Geometric description of a tree and corresponding voxel space.

Table 1
Average species parameters

	Value	
Geometric parameters		
D_0	1 cm	Initial dbh
D_{max}	150 cm	Maximal dbh
H_0	1 m	Initial tree height
H_{max}	40 m	Maximal tree height
S_H	150	Initial H/D ratio
R_0	0.5 m	Initial crown radius
S_R	7.0	(Crown radius/dbh) slope
h_0	0.5 m	Initial crown depth
S_h	0.1	(Crown depth/tree height) slope
Growth parameters		
ɡ	5 mm year^{-1}	Growth rate
D	3 m^2/m^3	Leaf density
P_0	0.2	Minimal p.n.a.
ϕ_c	10^{-2}	Minimal light level
M	1% per year	Mortality rate
H_c	1 m	Critical crown depth (see text)
Mechanical parameters		
C_0	2000	Average of C_c
C_1	$0.3C_0$	Variance of C_c
Fruiting/dispersion parameters		
A_m	10 years	Maturation age
T_f	1 year	Fruiting periodicity
N_s	30 seeds year^{-1}	Potential seedlings per year
ρ	40 m	Dispersal distance

The dbh D is the natural quantity available from field datasets. It is thus chosen in most individual based models as the basic descriptor of the tree growth. The dbh at age 0, D_0 is fixed at 1 cm. Other quantities should be related to D through simple relationships. As proposed by Rollet (1973) a linear crown radius–dbh relationship is chosen

$$R(D) = R_0 + a_R D \tag{2.1}$$

Parameters R_0 and a_R are species-dependent and are obtained from field data. The height–diameter relationship is widely documented for various forest types. Amongst the most used relationships are the quadratic law (Shugart, 1984) the exponential law (Prentice and Leemans, 1990; Pacala et al., 1996), the hyperbolic law (Kira, 1978; Gazel, 1983) and the power law (Lescure et al.,

1983; Moravie et al., 1997). Neither ecological nor theoretical arguments can provide a firm justification for the choice of one of these models. Furthermore, the quantitative difference between these curves is much smaller than the uncertainty on field measurements. Finally, no severe difference for these various choices are observed in simulation results. The hyperbolic law was used because it does not involve any transcendent function

$$\frac{1}{H(D)} = \frac{1}{H_{max}} + \frac{1}{s_H}\frac{D_{max} - D}{D} \tag{2.2}$$

s_H is the slope of the curve $H(D)$ around $D = 0$. Gazel (1983) gives $H_{max} = 49$ m, and $s_H = 196$ for a forest stand of French Guiana. Maximal tree heights range from 2 to 60 m depending on the species. Most rainforest trees have a flat crown architecture of the Troll type (Hallé et al., 1978), probably due to their strategy of optimal light interception. Therefore, we assume that $h \ll H$ and we take

$$h(H) = h_0 + s_h H \tag{2.3}$$

h_0 and s_h being new parameters. We are therefore left with only one variable, D, and simple relationships (2.1), (2.2) and (2.3) relating D to the other geometric variables of the tree.

2.2. Light availability

The computation of light availability is a critical step in TROLL since recruitment is mainly limited in the understorey by the fraction of the photosynthetically active radiation (p.a.r.).

Computing the local light level is all the more so complex because rain forest architecture is highly heterogeneous. A three-dimensional description of the light is proposed. The stand is discretised into volume cells, or *voxels* (Fig. 1), in which the leaf density is computed. In this approach light competition is not modelled via competition indices, but rather through the effective local light availability. If one wished to inspect every possible interaction among crowns directly one would have to perform more than 600 operations per tree. In TROLL the light field is computed first. Then this field is used in the tree

growth sub-model. This requires about 100 times less operations per tree than in the first method.

The basal area of each voxel is λ^2 so that the voxel space corresponds to the discretisation of the study area. However, the voxel height η is not necessarily equal to λ: vertical and horizontal discretisations are independent. It is suitable to take η lower than the minimal crown depth h_0. A leaf density d (leaf area per cubic meter) is defined for each species and measures the effective light interception capacity of a leaf layer. Field values give typically from 0.5 to 5 m^2 m^{-3} (Ashton, 1978) with a sharp decrease of the leaf density below the top of the crown. The effective leaf density $d(z)$ at a distance $0 < z < h$ below the top of the crown is simply modelled by an exponential relation (Fig. 2)

$$d(z) = d. \exp\left(-\frac{z}{h_c}\right) \tag{2.4}$$

where h_c is the critical crown depth and is to be compared to the maximal crown depth as defined in (2.3).

Let $d(x,y,z)$ be the sum of all the leaf densities for the trees found in the voxel of label (x,y,z). The leaf area index (l.a.i.) at point (x,y) integrated up to height z, $L(x,y,z)$. is thus simply defined by

$$L(x,y,z) = \sum_{z'=z}^{H_{max}} d(x,y,z') \tag{2.5}$$

Assuming a Beer–Lambert extinction law one finds that the light flux $\Phi(x,y,z)$ available just above the cell (x,y,z) is

$$\Phi(x,y,z) = \Phi_{ac} \exp\left[-k(L(x,y,z) - d)\right] \tag{2.6}$$

Φ is usually measured in moles of photons per second per square meter. An average value of the above canopy flux is $\Phi_{ac} = 2200$ µmol s^{-1} per m^2. For the sake of simplicity it is normalised to $\Phi_{ac} = 1$. k is the absorption rate per unit leaf density ($0.6 \le k \le 1.0$). This definition embodies the description of crown interactions. $\Phi(x,y,z)$ is used to compute trees light availability in the stand. Assume that (x,y,z) is a voxel in the crown of a given tree. If the tree fills the voxel alone then $d(x,y,z) = d$ so that there is no self-shading. However if two or more trees fill this cell then $d(x,y,z) > d$. In this latter case each tree sees a lower light intensity, therefore yielding a two-sided light competition. The average p.a.r. ϕ intercepted by a tree is computed on a tree with trunk located a point (x,y) from the field Φ, as shown in Fig. 2.

$$\phi(x,y) = \frac{1}{\pi R^2} \sum_{(x'-x)^2 + (y'-y)^2 < R^2} \Phi(x',y',H) \tag{2.7}$$
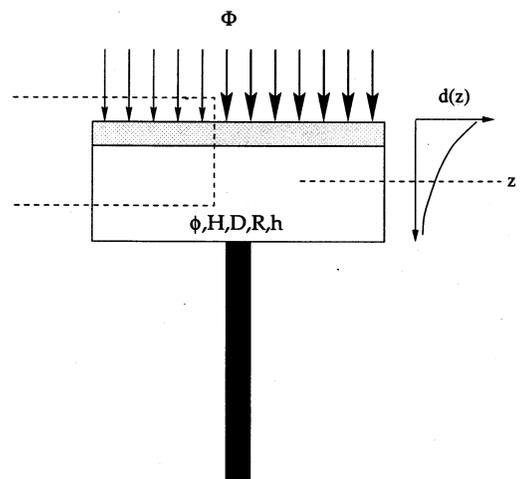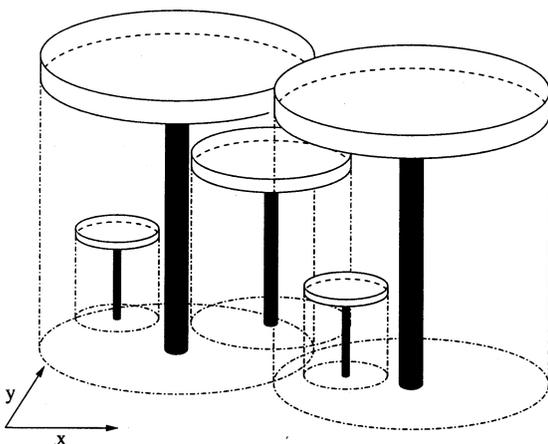
so that $0 \le \phi(x,y) \le 1$.

Fig. 2. Left: competition for light between trees. Complex shading patterns are shown. Right: light interception of the flux Φ and interaction with another crown (dashed). This crown lowers the flux ϕ intercepted by the tree. The leaf density decrease below the top of the crown (2.4) is also illustrated.
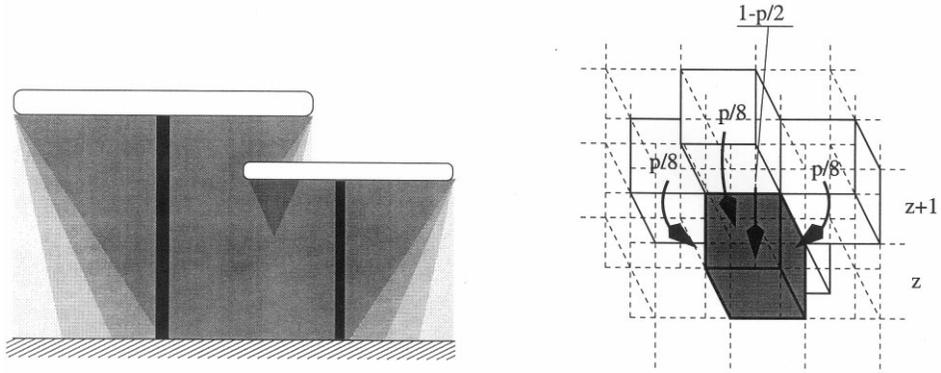
Fig. 3. Left: solar interception with angular-averaged radiation. Right: Computation of the l.a.i. field using Eq. (2.8).

It was implicitly assumed in this discussion that only overhead light radiation is significant. This is obviously an oversimplification although the seasonal light inclination is smaller on average in intertropical regions than in temperate regions. Sun flecks should indeed play a crucial role for understorey saplings. In treefall gaps, the assumption of vertical light radiation is equivalent to Brokaw's definition of a gap: a 'hole extending through all levels down to an average height of two m above ground' (Brokaw, 1982). As discussed by van der Meer et al. (1994) this definition underestimates the real regeneration surface (defined by Runkle, 1981 and Riéra, 1982) and therefore the regeneration capacity of the forest. To overcome this difficulty, the computation of the l.a.i. is slightly modified compared to Eq. (2.5) which assumes that $L(x,y,z) = d(x,y,z) + L(x,y,z+1)$ ((2.5) says that the l.a.i. only depends on the situation of the voxel just above). It is suitable to enrich this expression by including the action of nearest neighbour voxels. This raises the following expression

$$L(x,y,z) = d(x,y,z) + \frac{2-p}{2} L(x,y,z+1)$$

$$+ \frac{p}{8} \sum_{x',y'} L(x',y',z+1) \qquad (2.8)$$

where $(x',y',z+1)$ is one of the four nearest neighbour cells of $(x,y,z+1)$. The parameter $0 \leq p \leq 1$ controls the influence of non vertical radiation. For example $p = 0$ corresponds to only vertical radiation, while $p = 1$ corresponds to a radiation averaged over 90°. More precisely, the inclination from the zenith ψ, over which the radiation is averaged, is related to p through

$$\psi = \arctan\left(\frac{p}{2-p}\right) \qquad (2.9)$$

This method is illustrated in Fig. 3.

2.3. Tree dynamics

2.3.1. Establishment success

The first step in the tree dynamics is the establishment of newly germinated seedlings. This is managed through a seed bank defined at each discrete site (x,y) of the plot by an integer variable $\sigma(s|x,y)$, where s is the species label. The role of the seed bank in the regeneration dynamics of a tropical forest has long been acknowledged (Augspurger, 1984; Schupp, 1988; Raich and Gong, 1990). The major dynamic characteristics of this seed bank are modelled here. If there is no seed of species s at this site then $\sigma(s|x,y) = 0$. If at least one seed of species s is present, then $\sigma(s|x,y)$ is the age of the *youngest* seed. If $\sigma(s|x,y)$ is greater than σ_c, the dormancy age of a seed then the seed bank is emptied. Seed dormancy is characteristic of pioneer species, rather than of primary forest species (Richards, 1996). The above dynamic rules disregard any (positive or negative) density effect on a site (x,y). A seed succeeds if the site is free and if there is a sufficient p.a.r. level ($\phi > \phi_c$) for the corresponding species. In

this case, the seedling must grow up to the minimal dbh of 1 cm before being taken into account. The mortality rate is usually very high in the early life of trees and this assumption simplifies a lot the model. Several distinct biological phenomena (seed banks, seed dormancy, germination, early age growth), which all contribute to recruitment, are thus considered together in the establishment stage. The residence time in this early life stage could be very long especially for understorey species and therefore this residence time is introduced in the model.

If more than one species has seeds on the same site, the winning species is chosen at random among the possible ones. This does not mean that all species have the same recruitment rate since a strong competition occurs among trees in their early years. The recruitment rate is therefore controlled by environmental conditions.

2.3.2. Growth

The dynamics of a tree is related to the p.a.r. availability ϕ through the carbon potential net assimilation (p.n.a.) P. Typically, for C3 plants, the p.n.a. saturates around $P_{\max} = 25$ μmol s^{-1} per m^2 for $\phi > 2000$ μmol s^{-1} per m^2 with some differences between pioneer and climax species. Here, P is adimensionned so that $P_{\max} = 1$. P and ϕ are usually related by the Monod law

$$P(\phi) = \frac{\phi - \phi_c}{\phi + \phi_c/P_0} \qquad (2.10)$$

P_0 is the net respiration loss. ϕ_c is the compensation flux, that is the minimal light flux such that the photosynthetic fixation balances the photorespiration. ϕ_c is roughly related to the maximal value of the l.a.i., through $\phi_c \simeq \exp(-kL_{\max})$. A typical value of ϕ_c ranges from 1 to 3%, and $P_0 \simeq 0.2$. Note that values $P < 0$ are possible corresponding to a tree below the compensation point ($\phi < \phi_c$) or with a strong water deficit. As much as 12% of trees above 30 cm dbh can have negative size increments (Swaine et al., 1987a). The survival probability of such trees is very low (see below).

$P(\phi)$ is the net increment per unit time and per leaf area of the total biomass B. A very simple dbh growth equation was used

$$\frac{\mathrm{d}D}{\mathrm{d}t} = P(\phi)\mathrm{g}\left(1 - \frac{D}{D_{\max}}\right) \qquad (2.11)$$

where g is the dbh growth rate. This equation is a very good approximation of more complicated equations as long as the extreme values of D are not reached. Several other equations were tested in the form $D'(t) = D(t)^{\alpha}(1 - D(t)^{\beta})$ but they did not yield a markedly different behaviour for $\alpha = 0$, 1 and $\beta = 1,2,3$.

2.3.3. Death

The mortality is a probabilistic event related to the same external conditions as those ruling the growth, that is light availability. A simple way of accounting these environmental factors is to correlate the death rate m to the potential net assimilation P. Practically, a random variable μ distributed uniformly on [0, 1] is compared to the threshold

$$m_{\mathrm{eff}} = m^{-(P + P_0)/(1 + P_0)} \qquad (2.12)$$

where m is the residual mortality rate. A tree dies with probability m if P is maximal (i.e. $P = 1$). The tree dies if $\mu < m_{\mathrm{eff}}$. As expected $m_{\mathrm{eff}} \to 1$ as $P \to -P_0$ and therefore a tree dies with a high probability as the minimal p.n.a. is reached. A similar growth-dependent mortality rule was proposed for the SORTIE model (Pacala et al., 1996) and for the FORMIND model (Köhler and Huth, 1998) but the possibility of negative increments ($P < 0$) was not taken into account. Another cause of mortality is the phenomenon of treefalls the discussion of which is postponed to Section 2.5.

2.4. Seed dispersal

Fruiting strategies are highly variable in rain forests (Howe, 1983; Sabatier, 1985). Some species have periodic fruiting, others fruit only after external shocks such as a very dry season or in the senescent stage. Some species produce seeds only once in their lifespan, usually just before dying (monocarpic species). Finally, some species seem to present erratic fruiting patterns. To model these strategies, it is convenient to define some fundamental parameters such as the age of sexual maturity A_m, the fruiting periodicity T_f, the aver-

age number of produced seeds N_s and a probability distribution function for the dispersion length. These parameters are discussed below.

The maturity age A_m is discussed in Lieberman et al. (1985b). From their data, it is possible to estimate the time to grow from 1 cm dbh to the dbh at maturity, using the maximal estimated dbh increment. This yields a maturation age between 20 and 100 years which is only a rough estimate of A_m. Pioneer species can produce seeds at a younger age while some understorey species can wait more than 100 years before entering the mature stage (Charles-Dominique et al., in preparation). It was observed that fruiting events are seasonally correlated in some rain forests (Sabatier, 1985). Thus most trees fruit at least once a year ($T_f = 1$). However, this is far from being a strong rule.

Each mature tree produces a number of seeds which are dispersed in the neighbourhood, by different mechanisms (Charles-Dominique et al., 1981; Van der Pijl, 1982; Augspurger, 1984; van Roosmalen, 1985; Ribbens et al., 1994). The number of seeds per fruiting N_s varies from very few for understorey species to a huge number for pioneer species: for the pioneer *Cecropia* sp., as much as 10 seeds m^{-2} per day are dispersed by bats. The seed bank sub-model of TROLL assumes one seed per species and per space unit, the youngest one, since at most one tree can establish on this space unit. Ns is in fact the number of potentially established seedlings rather than the number of produced seeds. Therefore, field values should be lowered and N_s is in the range 1–100 in practice (one tree produces at most 100 offsprings per time step).

The average dissemination length from the parent tree is $\rho + R$, where ρ is the unique parameter here (R is the crown radius). The probability of a seed to be transported at the distance r from its parent tree follows a Gaussian distribution. The angle of dissemination is drawn uniformly between 0 and 2π. In two dimensions, the probability density for the distance r is

$$\text{Proba}(r) = \frac{2r}{(\rho + R)^2} \exp\left(-\frac{r^2}{(\rho + R)^2}\right) \qquad (2.13)$$

This choice is the simplest and the most natural. Indeed, the Central Limit Theorem insures that the Gaussian law becomes asymptotically valid for a large number of trials. Moreover rain forests are characterized by the low number of species disseminating their seeds by the wind (anemochorous transport) compared to small distance dissemination modes (zoochorous or autochorous transport). Actually more than 80% of Neotropical species are dispersed by animals (Estrada and Fleming, 1986). Although zoochorous dispersal can create rare events of an exceptional length, it is commonly assumed that the *average* dissemination length ρ is rarely more than 40 m (Dalling et al., 1998, reported a significant decrease for all species types beyond values of 30–60 m). For the distribution (2.13), 99% of the seeds fall at a distance less than $2.14(\rho + R)$ of the parent tree.

To model long distance dispersion modes, a nonlocal, density-dependent effect is also considered. The total number of mature trees of a given species is computed. The number of non-locally dispersed seeds is then proportional to the number of mature trees. These seeds are distributed randomly on the environment with no distance limitation. Both modes of dispersion are used to update the seed field $\sigma(s|x,y)$.

2.5. Treefalls

Treefalls are basically due to the falling of one tree but they can involve a large number of trees and they can cause strong perturbations locally (van der Meer et al., 1994). A simple method to describe treefall events consists in felling a tree at random. This method reproduces quite well observed statistics but it hides the basic mechanisms at their origin. Living trees can fall for at least three reasons. First, they are destabilized by their own architecture or because their roots are not well held (structural treefall). For example, they can be affected by wet soils (which loosen the hold of roots) and by steep slopes. Second, neighbouring trees may exert a destabilizing mechanical force (induced treefall). Third, they may be uprooted by a strong and sudden climatic perturbation like a storm, a hurricane or a landslide (external treefall). Felling a tree at random is

equivalent to considering only the first cause of treefall. Here, a sub-model is developed which encompasses the influence of neighbouring trees and takes into account climatic perturbations.

For each tree, the force **F** exerted by neighbouring crowns is computed. This is done by inspecting the tree crown. If the crown shares a voxel with another tree, then both are repelled (Fig. 4, left). Let $\mathbf{X} = (x' - x, y' - y, z)$ be the vector locating the voxel from the tree axe (x, y, z). The smaller $\|\mathbf{X}\| = \sqrt{(x' - x)^2 + (y' - y)^2}$ is, the stronger the force is

$$\mathbf{F}(x, y, z) = \sum_{\|\mathbf{X}\| < R} \frac{\mathbf{X}}{\|\mathbf{X}\|^2} \Theta(x', y', z) \quad (2.14)$$

where $\Theta(x, y, z) = 1$ if the voxel (x, y, z) is occupied by more than one crown, and 0 otherwise. The force intensity is $F = \|\mathbf{F}\|$. The mechanic influence on a given tree is proportional to its height which defines the mechanic couple $C = HF$, and the direction of the force, defined by the angle θ. In the somewhat different context of tree plasticity due to crown interactions, Umeki (1995) has proposed a similar model of a 2D force field with an interaction force scaling as $\|\mathbf{X}\|^{-1}$.

Trees fall only if the couple C is greater than a threshold value in the absence of any external mechanical destabilizing effect. Each tree is then characterized by a mechanical stability threshold C_c depending on both the tree species and its environment. For example, Henwood (1973) proposes that buttressed trees are less susceptible to fall; yet there is no clear evidence of this fact from

field measurements (Young and Perkocha, 1994). To take into account structural effects, we define C_c as a random variable distributed following a Gaussian law of average value C_0 and of variance C_1. As soon as $C > C_c$ the tree falls in the direction θ. C_0 evaluates the importance of mechanic tree interactions, while C_1 evaluates structural factors-in particular the hold of roots (Jeník, 1978; Oldeman, 1990).

When falling, the tree destructs neighbouring individuals in the direction θ (Fig. 4, right). Other neighbouring trees can be destabilized by the modification of the local force field during the following time steps. This is what Riéra (1982) calls 'chablis multiple' (multiple treefall). This process needs no further modelling since it is already encompassed in TROLL.

The influence of the climate on treefall events can also be taken into account. It has been observed (Brokaw, 1984; Riéra and Alexandre, 1988) that important rainfall increases the weight of the crown by up to a factor two, and therefore lowers the mechanical stability threshold C_c Also, the action of wind is equivalent to adding a constant drift force $\mathbf{F}_{wind}$ to **F**. Lastly, if the tree grows on a steep slope, uprooting is likely to be favoured, though this hypothesis remains largely unclear (Herwitz and Young, 1994; Condit et al., 1995a).

The action of treefalls as modelled in the present study is not directly related to field data. The maximal couple intensity is proportional to $H_{max} h_{max} R_{max}^2$; this is easily understood if one
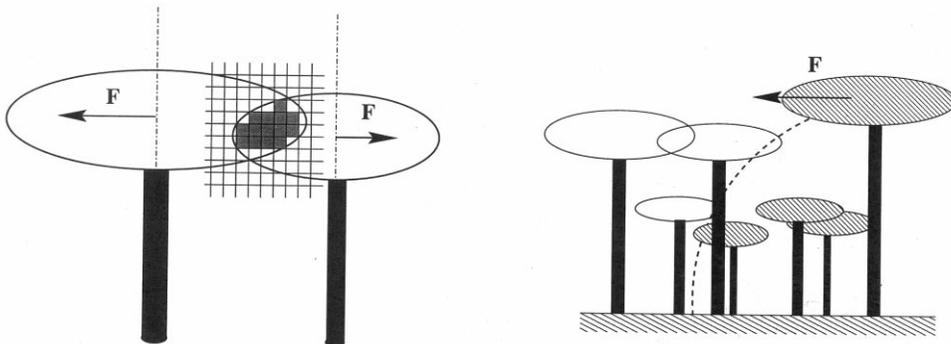

Fig. 4. Treefall model. Left: the strength of interaction is proportional to the number of shaded voxels. Right: indirect destruction of trees by the falling of a tree. Shaded trees are killed by the treefall.
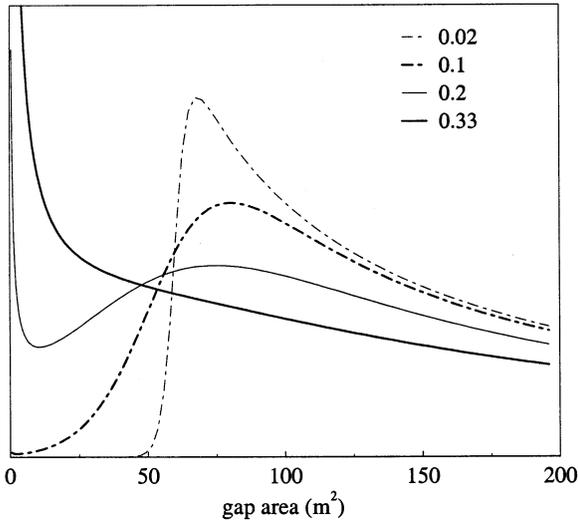
Fig. 5. Predicted number of treefalls creating a gap of given area. A power-law decay of the stem number per dbh is assumed, for various values of C_1/C_0. If $C_1/C_0 \ll 1$, only large gaps can exist while if $C_1/C_0 \simeq 1$ all trees fall with an equal probability. The number of treefalls is normalized.

takes two trees at a minimal distance and with maximal height and crown radius. Then the force is proportional to $h_{max}R_{max}^2$. Consequently if $C_1 = 0$ a treefall occurs as soon as $C_0 < C_{max}$. In this situation treefall gaps are all large in size, since only trees such that $hHR^2 > C_0$ can fall. The inter-individual variability C_1 smoothes this effect. The effect of C_1 on the treefall gap size distribution is shown in Fig. 5. For small C_1 only large treefalls can occur (circles). For large C_1, small treefalls are also observed. To account for the observed form of the size class distribution of treefall gaps (Brokaw, 1982; Chandrashekara and Ramakrishnan, 1994; van der Meer et al., 1994; Riéra, unpublished), high variability $C_1/C_0 = 0.3$ is chosen.

3. Performances, parameterization and sensitivity

The modules presented in this article require a large number of elementary operations. Hence, it is difficult to access large simulations — and statistically significant outputs — on classical computers. Simulations are then run on a network

of processors sharing some information and making the time consuming operations in parallel. For the present work, a source code (available upon request) was written in C + + language, and a Cray T3E machine with 288 parallel DEC-Alpha processors was used. Each processor simulates only a strip of the total plot. We have been able to simulate plots of size 20 km^2, that is up to 2×10^7 stems.

3.1. Parameterisation

Parameterization is the crucial step in the development of a forest model. It is especially so in the case of species-rich forests where very few complete forest datasets are available. We must reduce the number of free parameters. This is done first by grouping species into plant functional types, and then by finding the confidence interval of each of the remaining parameters with the help of field data. To find a set of parameters we have proceeded by trial-and-error controlling a few global output data (stem density) and checking the consistency of the parameters with other outputs (basal area, density of the different groups).

In most modelling approaches for rain forests, species are grouped into functional types (for more conceptual justifications, see Vasquez-Yanes and Guevara-Sada, 1985; Swaine and Whitmore, 1988; Köhler et al., 1999). Two main functional types are usually defined with respect to the light demand strategy of seedlings: light demanding species (LD) and shade tolerant species (ST). Typical LD families are the Cecropiaceae in the Neotropics, genus *Musanga* (Cecropiaceae) in Africa and genus *Macaranga* (Euphorbiaceae) in Asia. Typical ST species are the Sapotaceae and Caesalpiniaceae in the Neotropics, genus *Entandophragma* and *Khaya* (Meliaceae) in Africa and the Dipterocarpaceae in Asia. Here we add an intermediate light demand group (called I) grouping species whose seedlings can develop both in the understorey or in canopy openings.

Using the maximal tree height H_{max} we further discriminate the species into height groups. For the purpose of the present work, a grouping for old forest stands is shown (Table 2) which roughly reflects the situation in Neotropical rain-

Table 2
Main parameters for the species grouping in French Guiana

Species type[a]	Species number[b]	L.a.i.[c] max	P.n.a. min	M (% per year)	A_m (year)	N_s	ρ (m)	$\mathfrak{g}$ (mm yr^{-1})	D_{max} (m)	H_{max} (m)	R_{max} (m)
LD1	21	4.8	0.08	4	5	150	60	2.24	0.07	5	1.76
LD2	104	4.8	0.08	2.5	10	120	50	4	0.2	15	3.5
LD3	52	5	0.08	2	15	105	40	6.4	0.4	25	6.1
LD4	44	5	0.1	2	20	75	40	9.6	0.6	40	7.7
I1	13	6	0.12	2.2	12	60	40	1.76	0.1	5	2.1
I2	72	5.8	0.12	1.4	20	50	40	2.46	0.22	14	3.58
I3	83	5.6	0.12	1.4	25	40	40	4.48	0.4	23	5.3
I4	96	6.4	0.12	1.4	40	24	40	8.96	0.8	40	6.9
ST1	151	8	0.22	1.4	20	32	20	3.36	0.3	5	5.3
ST2	148	7	0.2	1.2	30	16	20	4.8	0.5	15	7.5
ST3	116	7	0.2	1	40	10	20	7.2	0.9	25	11.3
ST4	122	7	0.2	1	50	8	20	9.6	1.2	50	10.1

[a] LD, light demanding; I, intermediate; ST, shade tolerant.
[b] Number of species in each group for the French Guiana rain forest.
[c] L.a.i. max. is related to the minimal light availability ϕ_c through $\phi_c \simeq \exp(-kL_{max})$ and the minimal p.n.a. is noted P_0 in the text.

forests of French Guiana where the light demand type and maximal height have been collected for more than 1000 tree species (Chave et al., in preparation).

The present species grouping uses three light demand types (LD, I and ST) and four height classes (0–5 m, 6–15 m, 15–25 m and 25–50 m) as shown in Table 2.

Once this work is performed, we fix the confidence interval for the $16 \times 12 = 192$ parameters of the model using field data. We give here a restricted and by no means exhaustive report of

relevant data for the dynamic parameters of a tropical forest model (Table 3). See similar tables in Putz and Milton (1982), Lieberman et al. (1985a), Pélissier and Riéra (1993), Swaine et al. (1987b) and Phillips et al. (1998).

The minimal death rate m is a lower bound of the actual death rate m_{eff}. Average values of the mortality are observed in the range 0.2–10% per year (Table 3). The value of m is correlated to that of the dbh growth rate $\mathfrak{g}$ since the product

$$\Omega = (D_{max}/\mathfrak{g})m$$

Table 3
Growth and mortality rates from field measurements

Country	Reference	Study area (ha)	Period	Stem number	Minimal dbh	m (% per year)	$\mathfrak{g}^a$ (mm year^{-1})
Panama	Condit et al. (1995a)	50	1982–85	235 895	1 cm	2.75	—
Panama	Condit et al. (1995a)	50	1985–90	242 218	1 cm	1.98	—
Panama	Lang and Knight (1983)	1.5	1968–78	4668	2.5 cm	2.00	2.47
Costa-Rica	Lieberman et al. (1985a, 1990)	12.4	1969–82	5622	10 cm	2.03	2.65
Ecuador	Korning and Balslev (1994)	4.1	5 yrs	2655	10 cm	2.30	2.7
Peru	Gentry and Terborgh (1990)	0.943	1974–84	567	10 cm	1.6	—
Fr. Guiana	Pélissier and Riéra (1993) Riéra (1995)	1.78	1981–91	2088	5 cm	1.07	1.35
Fr. Guiana	B. Riéra, unpublished	10	1989–91	3440	10 cm	1.04	1.75
Fr. Guiana	Gazel (1983)	8	1968–78	2114	15 cm	1.46	3.73
Fr. Guiana	Gourlet-Fleury 1997)	—	1984–94	3157	10 cm	1.09	1.26
Fr. Guiana	Gourlet-Fleury 1997)	—	1984–94	3986	10 cm	1.44	2.11[b]
Brazil	Manokaran and Kochummen (1987)	5	1981–86	3125	10 cm	1.16	—
Malaysia	Rankin-de-Merona et al. (1990)	2	1947–81	1075	10 cm	2.02	2.49
Ghana	Swaine et al. (1987a)	2	1968–82	1103	10 cm	1.76	1.09[c]
Australia	Herwitz and Young (1994)	0.4	1982–92	112	30 cm	1.7	2.7

[a] $\mathfrak{g}$ is the overall average growth rate.
[b] Reduced impact logging (10 stems ha^{-1} more than 50 cm dbh).
[c] Estimated.

should be roughly constant. Otherwise, TROLL would overestimate the number of large trees in the case $\Omega \ll 1$ or only small trees with $D \ll D_{\max}$ in the case $\Omega \gg 1$. Both situations should be avoided and the lifespan of a tree is related to its growth time. Thus higher dbh growth rates correspond to higher mortality rates. It is observed that $\mathfrak{g}$ shows a large interspecific variability (from 0.3 to 15 mm year^{-1} on average) and a size dependence. This is evidenced on average growth rates which are systematically higher when small individuals are discarded. For trees below 5 cm dbh, one has $\mathfrak{g} < 1$ mm year^{-1}, while for trees above 30 cm dbh, $\mathfrak{g}$ is often more than 5 mm year^{-1} (with a decrease in the senescent stage). This observation is consistent with the criterion $\Omega \sim 1$. In practice, the *optimal* growth rate $\mathfrak{g}$ — that is without the limiting effect of shading — is taken in the range 1–20 mm year^{-1}.

These data are used to construct a first dataset. Then, a series of runs are performed to scan the allowed region of the parameter space. The lists of parameters raising compatible results in terms of number of trees above 1, 10 and 30 cm, and in terms of basal area are kept. The classically reported field data for the total basal area are usually between 25 and 65 m^2 ha^{-1}. They strongly depend on the number of large trees in the stand. The number of large trees per hectare is also frequently reported since it is quite easy to measure in the field. The number of trees above 10 cm dbh ranges usually between 400 and 700 stems ha^{-1} and the number of stems above 30 cm dbh ranges between 60 and 150 stems ha^{-1}. The mortality rate is roughly of 1% per year (trees above 10 cm dbh) half of which is due to treefalls. Table 2 is one of these lists.

3.2. Sensitivity analysis

A preliminary set of runs was performed to test the different modules of the code. A special care was taken in quantifying the influence of light field discretisation in both horizontal and vertical directions. Figure 6 (upper, left) shows the effect of varying the vertical step η on the average l.a.i. at various heights above the ground. The use of a finer mesh grid increases the quality of the result,

especially for lower canopy layers. However the computation time increases too.

Figure 6 (upper, right), one observes that the dynamics of TROLL is not drastically modified by the variation of the horizontal mesh grid λ. The stem density decreases at small λ due to small-scale treefalls. Conversely, large λ values yield larger discretisation errors which also decrease the stem density. It is thus reasonable to preserve $\lambda = 1$ m. age as well as the seed production are therefore tuned quit precisely in Table 2 for example. The influence of non vertical light incidence was also tested. The result on the density of stems above 1 cm dbh is given as a function of the maximal light incidence angle (Fig. 7).

A singular behavior is observed for $\psi \simeq 0$ (see Eq. (2.9)); the stem density scales approximately as $\psi^{1/4}$). However, the non-equilibrium dynamics is not modified and choosing $\psi > 0$ results merely in shifting the stem density upwards.

As pointed out by Vanclay and Skovsgaard (1997), validating each module of a forest growth model is not sufficient. Even simplified guideline such as analytic solutions is not available. In all the tests we prepared an equilibrium state and then we varied some parameters in order to control the resilience of this equilibrium. Starting with one species group from the average values presented on Table 1, the parameters were independently varied. The results of these tests are not reproduced here, but the variation of the stem density with growth rate $\mathfrak{g}$ and the mortality rate m (Fig. 6) are shown. Figure 6 supports the consistency requirement $\Omega \sim 1$ since increasing $\mathfrak{g}$ looks equivalent as decreasing m. Increasing the mortality increases the stem density because it favours the establishment of a large number of young trees.

It is observed in these runs that the results smoothly depend on the growth/death parameters and on the geometric parameters (maximal height, maximal dbh, …). We have also observed that the results are very sensitive to the parameters of the regeneration module. This is not surprising because regeneration is the crucial step in the maintaining of a species group. The age of maturation and the seed production both control the maximal
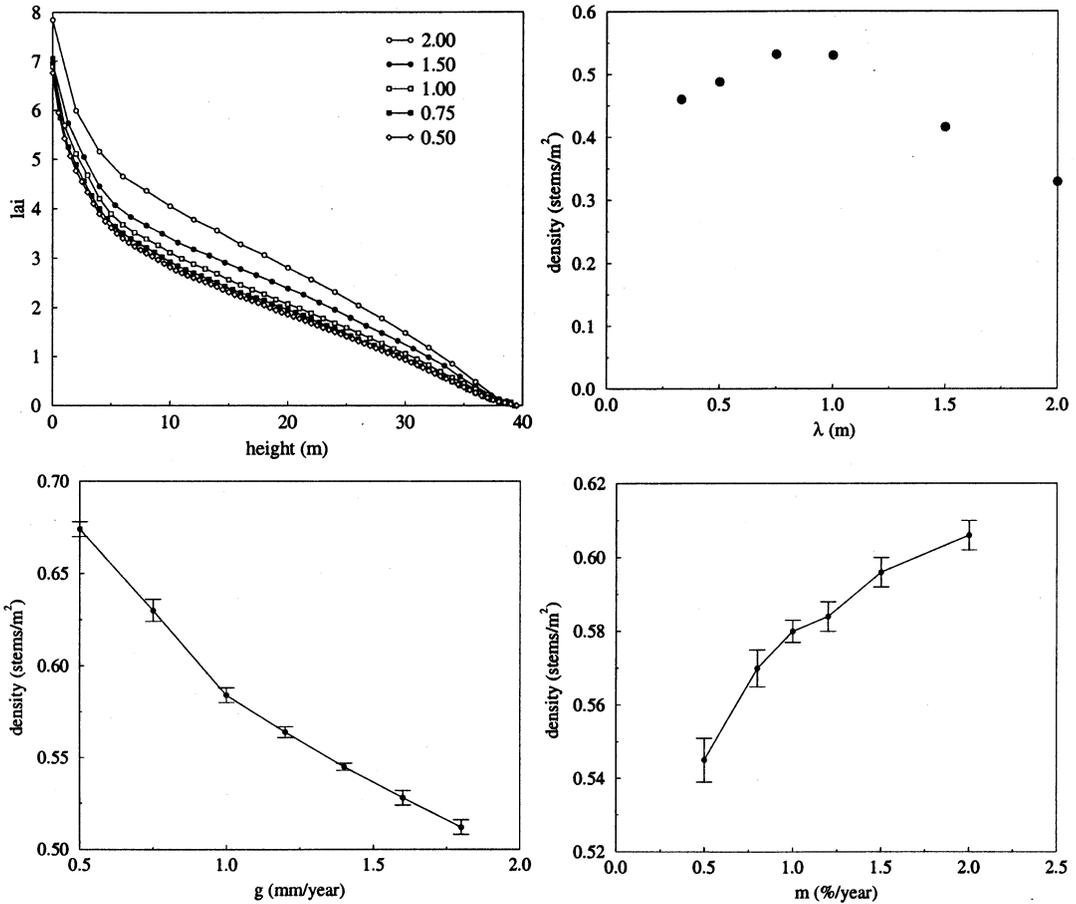
Fig. 6. Upper, left: average l.a.i. over voxel layers is plotted for five values of the vertical discretisation step η between 0.5 and 2 m. The sharp increase at lower canopy layers is due to the presence of trunks. Upper, right: Equilibrium density of stem (dbh > 1 cm) for six values of the horizontal discretisation step λ between 0.33 and 2 m. Lower: variation of the growth rate (left) and of the mortality rate (right) on the total stem density. Forest stand of 160 ha after equilibration (500 years) with one species.

reproduction rate per year through the ratio N_s/A_m.

The treefall sub-model needs an independent study. Let us turn it off to evaluate the influence of treefall clearings on the regeneration dynamics. The mechanism of stand replacement, described by Moravie et al. (1997), is dominant in this case. We show the ground level l.a.i. in Fig. 8.

With the treefall model switched on, gaps are clearly visible and induce a great heterogeneity. Only one large sized species is present in this test, therefore the typical gap size is exaggerated. A plain consequence of the absence of treefalls should be the disappearance of the LD species.

This is confirmed by runs including one LD and one ST species. The stem density of LD species as a function of that of ST species is plotted in Fig. 9.

This phase space representation allows one to clearly appreciate the disappearance of LD trees in the absence of treefalls (circles), while the system reaches a stationary point with treefalls (Fig. 9, left, inset). The number of treefalls per hectare as well of the maximal couple in the plot are both computed at each time step (Fig. 9, right). It raises values slightly greater than field observations (Chandrashekara and Ramakrishnan, 1994, compiled seven field studies which give values
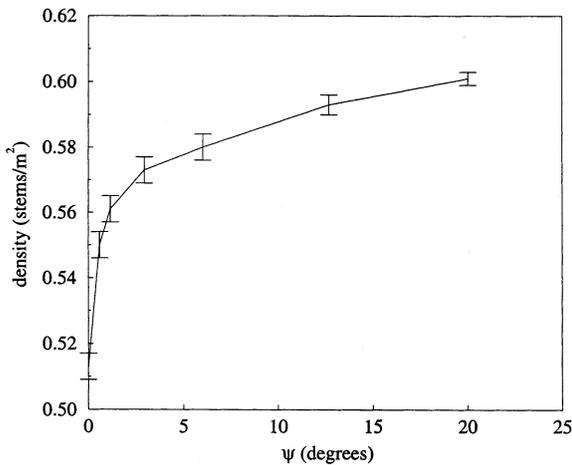
Fig. 7. Influence of the angular radiation. Forest stand of 60 ha after equilibration (400 years) with one species.

from 0.5 to 1.21 gaps ha^{-1} per year). However, one treefall event does not necessarily yield a novel gap since trees can fall on already formed gaps (multiple treefall). In consequence, the variable presented in Fig. 9 naturally overestimates the gap number. Then we conclude that the treefall model reflects quite well the real dynamics.

4. Applications

Three types of experiments are done with the TROLL tropical rainforest simulator. We study the

structure of the dbh size distribution, successional patterns and invasion of a plant community.

4.1. Tree population structure

The forest structure is often characterized by the dbh size class distribution $N(D)$ (Rollet, 1973) for which a lot of field data are available. They generally indicate a power law decay $N(D) \sim D^{-\delta}$, or an exponential decay $N(D) \sim \exp(-aD)$. Several measures in Malaysian dipterocarp forests were reported and yielded a power law with $\delta = 2.88$ (Appanah et al., 1991) or $\delta = 2.45$ with bins of width 1.6 cm and $\delta = 2.60$ with bins of width 3.2 cm (Newbery et al., 1994). Data in French Guiana (Fig. 10, left) show an apparent crossover between two behaviors for small dbh and for large values. In the range 10–50 cm a power law is observed with $\delta = 2.39 \pm 0.05$, while large values (30–100 cm) are more consistent with an exponential decay.

The dbh size class distribution is simulated in TROLL. It is plotted with a bin width of 1 cm and for a forest stand of 640 ha during 500 years and only for one 'average' species (Fig. 10 right). The actual exponent is in fact slightly *lower* than 2 (this fact was systematically observed in simulation results). This observation does not fit with field observations. One reason for this
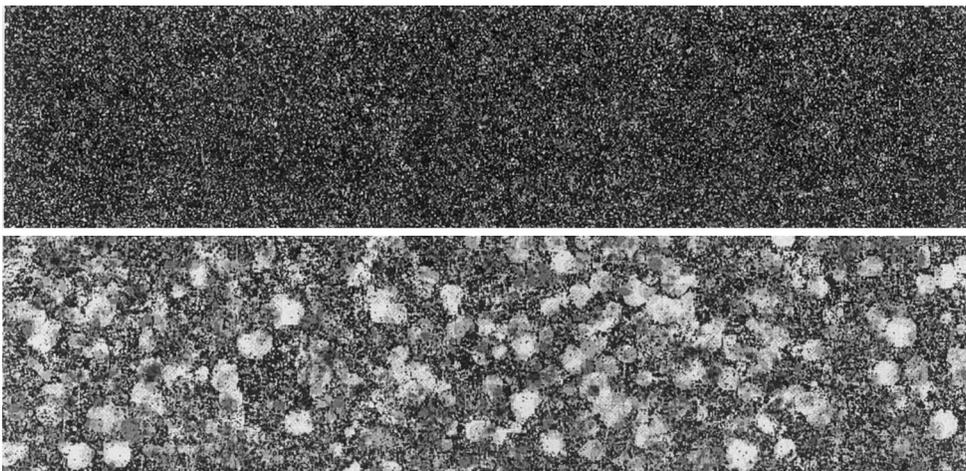

Fig. 8. Two dimensional l.a.i. field at the ground level. Upper: without treefalls. Lower: in the presence of treefalls. Color map from white (l.a.i. = 0) to black (l.a.i. > 7). Plot of 800×200 m, one pixel per m^2.
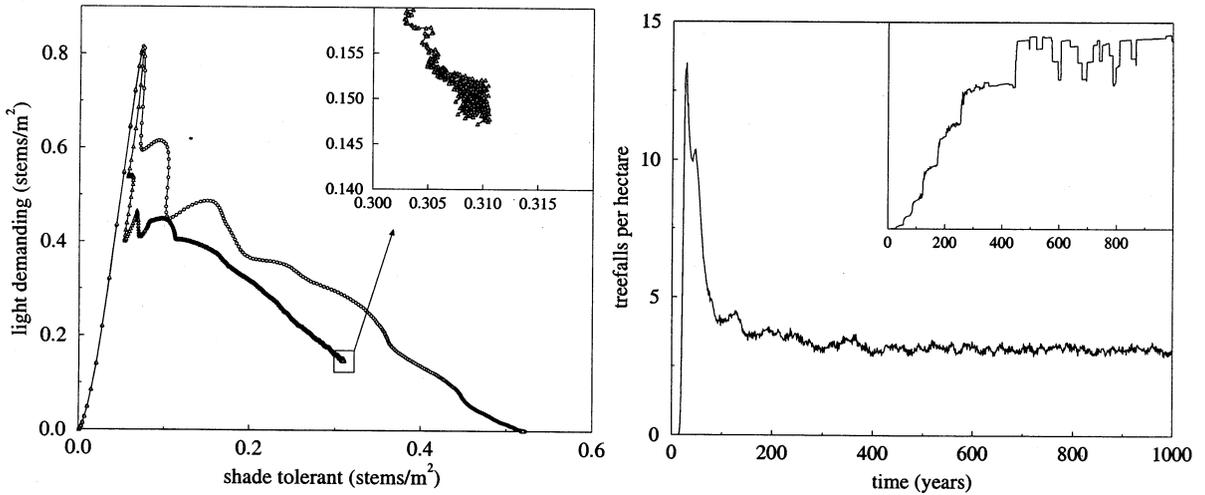
Fig. 9. Left: stem density of a light demanding species as a function of the stem density of a shade tolerant species. The two curves correspond to absence of treefalls (○) and presence of rare treefalls (△). In the absence of treefalls, light demanding species completely disappear, while with treefalls, coexistence occurs (see inset). Observe the damped oscillation pattern due to the low number of simulated species types. Right: average number of primary treefall events (inset: maximal intensity of the mechanical force exerted on trees computed in the stand, in arbitrary units). Results from a simulated plot of size 250 ha during 1000 years.

discrepancy is that the bin width chosen in field studies may alter the curve shape as clearly evidenced in the work of Newbery et al. (1994): the exponent δ *decreases* with the bin width. Moreover, it is obvious that the diversity of vegetation types in real forests might alter the result. We then used the parameterization with several plant functional types (Table 2) to assess this latter hypothesis. The resulting distribution $N(D)$ is also shown in Fig. 10, right. The curve shows a power law behaviour for small dbh values. If one focused in the range 10–200 cm (inset), it would be tempting to overestimate the power law exponent. Indeed, a fit of the curve in the region gives $\delta = 2.81$ with a good accuracy, close to field and other simulation results (Bossel and Krieger, 1994). Therefore it is reasonable to suggest that the power law behaviour $N(D) \sim D^{-2}$ is typical of monospecific forest stands with completely closed canopy layers. The species-diverse character of forest stands does alter this situation.

To understand the possible physical origin of the power-law behavior, we use the model due to Slatkin and Anderson (1984). It is a very simplified approach of space competition, which is analytically solvable. One assumes that a tree

crown grows linearly until it touches another tree crown in the same canopy layer (i.e. of the same size). At this stage, one of the two trees dies. This model yields $\delta = 2$, since the number of surviving trees is optimized at each canopy layer independently of the other layers. This exponent can be understood as a particular formulation of the self-thinning law. In general, the departure from this value is the signal of size class interactions. It is worthwhile noticing that if one assumes that each canopy layer has a depth h proportional to the tree height H, then the above self-thinning argument gives $DN(D)$, rather than $N(D)$. Hence, $DN(D) \sim D^{-2}$ and therefore $\delta = 3$, which should be an upper bound for δ. Gazel (1983) proposed a fit of his data similar to

$$N(D) = \frac{a \exp\left(-(D/D_0)^2\right)}{1 + cD^2} \tag{4.1}$$

which is plotted in Fig. 10. This is a very interesting point since the power law exponent $\delta = 2$ is recovered for $D \ll D_0$, while a sharper decrease is observed as $D \ll D_0$. Moreover, theoretical considerations fit well with this view which can be seen by defining a multi-species version of the Slatkin–Anderson model. Vertical competition of the lay-

ers as well as the low probability for trees to grow above the lower layers both result in a cut-off D_0 in the distribution $N(D)$.

4.2. Succession dynamics: the forest cycle

A succession scenario is simulated in the presence of treefalls. It consists of a 1000 ha forest stand with the species grouping described in Table 2 and starting from an empty initial condition. This run is performed during 1000 simulated years. The savanna type invades the area very fast (up to 50% of the cells are occupied in 5 years). Then it is out-competed by pioneer groups which reach their maximal occupancy between 15 and 50 years. Following this fast invasion (less than 100 years) a slow maturation process settles in the main actors being intermediate and shade tolerant species. Intermediate species are dominant in all forest strafes after 100 years of simulation (Fig. 11A,B). Then, a very slow succession leads to the dominance of shade tolerant species after 500 years for stems above 1 cm dbh (Fig. 11A) and 700 years for stems above 10 cm dbh (Fig. 11B). Pioneer species never disappear and form as much as 12% of the stems at the end of the simulation.

The over-representation of large trees (220 ± 10 stems ha^{-1} above 30 cm dbh), results in large values of the basal area which is above 60 m^2 ha^{-1} after 1000 years of simulation (Fig. 11C).

It is worth mentioning that while the stem density reaches is equilibrium value in a few years (about 50 years), the basal area shows a much slower dynamics due to the slow growth rate of large shade tolerant trees. This phenomenon is even more important for the biomass. To better understand the maturation process, the stem density was summed over groups with the same maximal height, irrespective of their light demand (Fig. 11D). It is observed that the dominant group is that of lower mid-storey species with maximal height H_{max} between 5 and 15 m, followed by small species (less than 5 m), upper mid-storey species (between 15 and 25 m) and canopy species (more than 25 m). This order is not modified in time, except in early succession stages when small species are dominant.

The population dynamics reflects well field results. These values are consistent with most observations in tropical rainforests. In the simulation, we find 4100 ± 10 stems ha^{-1} above 1 cm dbh, 930 ± 10 stems ha^{-1} above 10 cm dbh and $220 \pm$
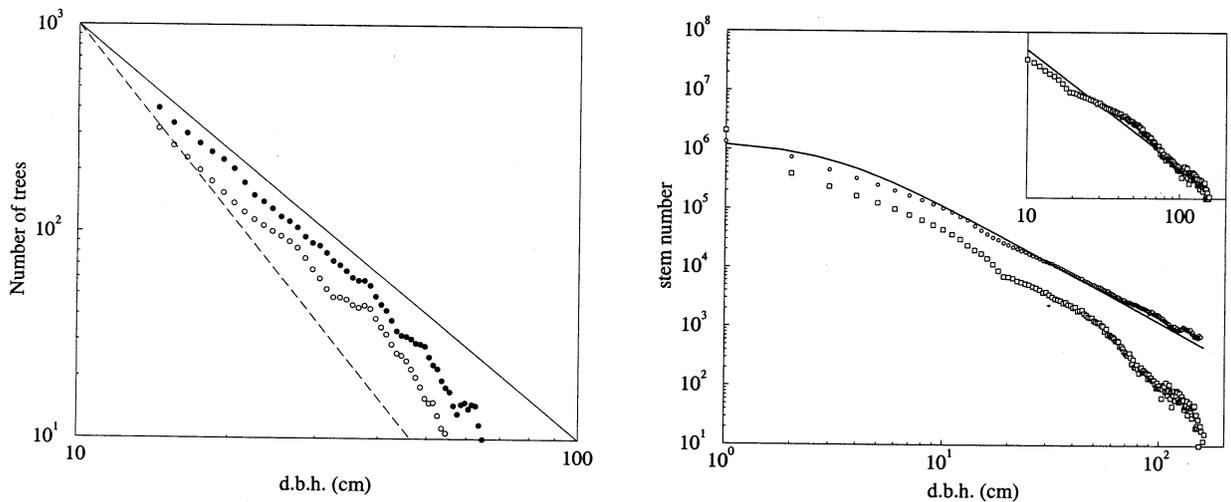

Fig. 10. Left: dbh size class distribution for two forest stands in French Guiana. o: 3440 trees over 10 cm dbh (research station Piste de Saint-Elie). ●, 5321 trees over 10 cm dbh (research station les Nouragues). Curves D^{-2} (solid line) and D^{-3} (dashed line) are plotted for reference. B. Riéra, private communication, and Riéra (1995). Right: simulation results with one species (○) and with 20 species (square), inset: magnification of the distribution for 20 species in the region 10–200 cm and fit by a power law (slope 2.81). Simulation of a 800 ha plot during 500 years.
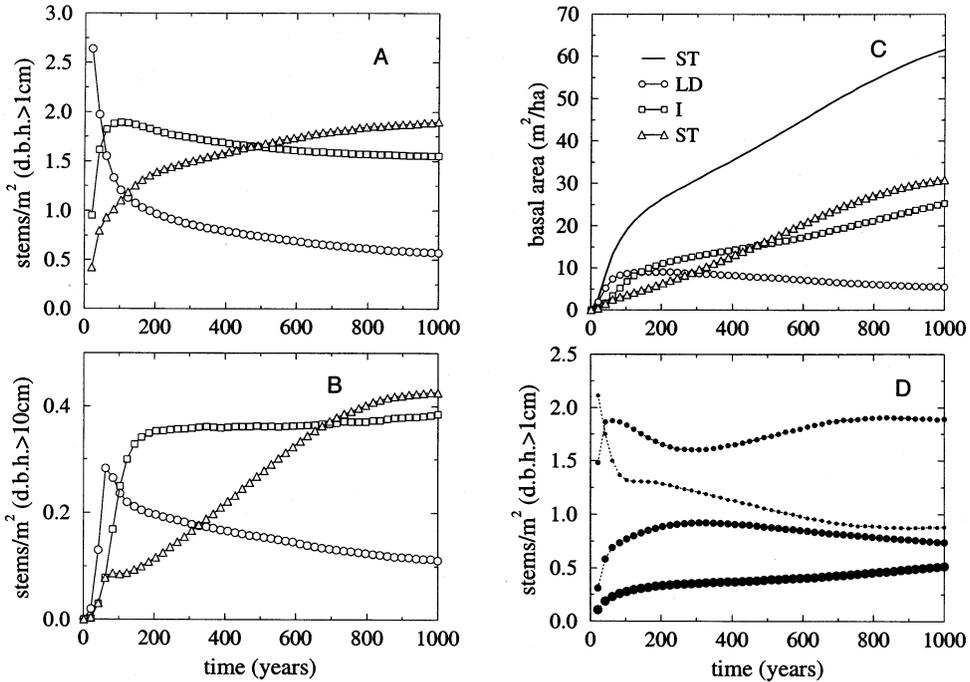
Fig. 11. Succession scenario from a clear-cut area. Parameterization given in Table 2 is used for a of size 500 ha during 1000 years. Average number of stems above 1 cm dbh (A) and 10 cm (B) and average basal area (C) for the three light demand groups. D: average number of stems above 1 cm dbh for the four height groups, with maximal height less than 5 (small ●), 15, 25 and 50 (big ●).

10 stems ha^{-1} above 30 cm dbh at the end of the simulation. The juvenile stages show a high mortality. In the installation phase the overall mortality is over 50% per year. Then the light-induced and natural mortality decreases to around 42% per year. Treefalls also have an effect on small trees and saplings. A the end of the simulation, the treefall-induced death rate is about 12% per year. For large trees (above 10 cm dbh), the mortality rate is around 2% per year with about 1.5% per year due to natural death and light competition, and 0.5% per year due to treefalls. The frequency of treefall gap formation reaches about one gap per year in the late succession stage, in accordance with field results.

4.3. Spatial dynamics

We now turn to the study of spatial patterns in tropical rain forests. We take the same plot and the same parameterization as in the last subsec-

tion but initially the seeds are placed in the 200 m of the leftmost part of a 4000 × 500 m forest transect (see Fig. 12). The rest of the transect is completely sterilized (all seed banks are empty and no tree is present initially). In this case, regeneration is limited mainly by seed dispersal. We have switched off the non-local dispersal mode — which physically corresponds to wind-dispersed seeds for example — to better understand the small distance effects. The density of each group is measured in square plots of size 50 × 50 m each, every 10 years. Figure 12 shows the stem density averaged along the stripe for trees above 10 cm dbh and for three different time steps.

After 100 years of simulation, about 2 km have been invaded and almost 600 m are in a pioneer forest with (corresponding roughly to a density less than 300 stems above 10 cm dbh ha^{-1}). The LD (pioneer) invasion front is about 100 m large.

The old growth forest takes place in the first 200 m, and between 200 and 900 m, a mixed forest type (above 300 stems ha^{-1} but below 500 stems ha^{-1}) is encountered. One hundred years later, the pioneer front have moved rightwards to 3700 m from the origin, the mixed forest front is at 2000 m but the old growth forest front is only at 350 m. Thus, the invasion speed of the pioneer forest is about 20 m year^{-1}, that of the mixed forest is about 10 m year^{-1}, but for the old growth forest, this value drops to c.a. 1.5 m year^{-1}.

5. Discussion

The TROLL model reproduces the structural properties of a rain forest stand. Due to the large number of simulated trees we can compare the theoretical diametric distribution due to Slatkin and Anderson and that obtained with our more detailed approach. Trees below 10 cm dbh follow theoretical predictions and the singularity D^{-2} is clearly evidenced the simulation results. The suc-
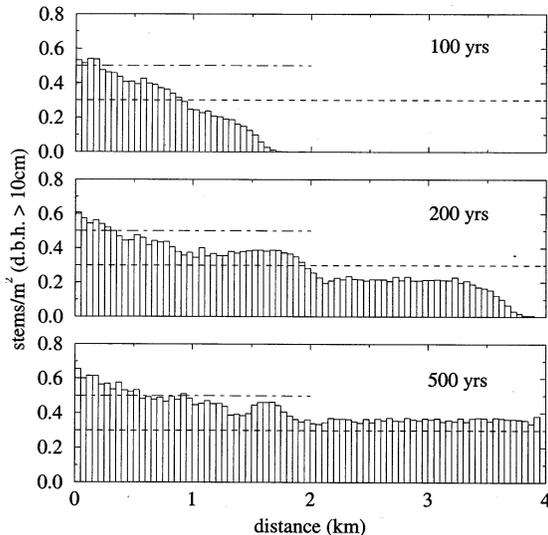

Fig. 12. Simulation of a tropical rain forest invasion front. The stem density above 10 cm dbh is used as an indicator of the forest type. Three fronts are clearly present corresponding (from right to left) to the pioneer forest front, the mixed forest front and the old growth forest front.

cession scenario presented here deserves a further discussion. Köhler and Huth (1998) have recently proposed simulation results of a primary dipterocarp forest of Sabah, Malaysia (Borneo) during 500 years using the FORMIND model. Starting from a clear-cut as in the present work, they find that an equilibrium state is reached after about 200 simulated years. This is in conflict with the simulation using TROLL, where a fast invasion phase of about 50–100 years, with a significant number of pioneer trees, is followed by a maturation phase with much slower trends reflecting the competition between the different plant functional types. This difference comes from the presence of a feedback due to seed bank limitations which are absent in FORMIND. The mature phase strongly depends on the recruitment capacity of shade tolerant species. Whether this slow dynamics is meaningful or whether it is negligible compared to the influence of climatic perturbations over several centuries is still a questionable issue.

In regard of the very rapid spread of tree communities in temperate regions after the last glacial maximum, the velocity of the pioneer front (~ 20 m per year) seems underestimated in our simulation results. Two distinct theories resolve this issue. Eq. (2.13) should be replaced by a long-range (Lévy-like) probability distribution function to account for long distance dispersal. Alternatively the preservation of micro-refuges during arid or cooler past periods could have significantly enhanced the spread speed. While the first hypothesis is the most probable in boreal regions—it is difficult to figure out how a micro-refuge could have persisted in the last Ice Age in the Northern part of Europe — the situation is much less obvious in inter-tropical regions. The large size of tropical plant seeds and the possibility for relict forests to persist along rivers both plead for the second hypothesis.

The slow migration of shade tolerant species can be detected in the field. For example, several Guianan species with heavy seeds, mostly scatter-hoarded by rodents, such as *Eperua falcata*, *Eperua grandifora*, *Vouacapoua americana* Caesalpiniaceae, (Forget, 1988) or *Astrocaryum sciophilum* Arecaceae (Charles-Dominique et al., in preparation) present a clustered spatial distribution which

may result from the influence of past dry events in this region (ECOFIT project; Servant et al., 1993; Bush, 1994; Charles-Dominique et al., 1998). TROLL is a new way to study such slowly dispersing species, which is almost impossible with other models. In the present simulation, the predicted value of 1.5 m per year for the old-growth forest invasion front is consistent with $\delta^{13}C$ dating in the Mayombe forest, Congo (Schwartz et al., 1996; Chave et al., in preparation) and with the spread velocity of the palm *Astrocaryum sciophilum* in French Guiana (Charles-Dominique et al., in preparation). A related issue is that of small-scale speciation phenomena (Gentry, 1989; Bush, 1994). Since trees are both individually modelled and physically located in large stands, cross-pollination sub-models and genetic drifts can be incorporated as done in the work of Doligez and Joly (1998).

In conclusion, this model provides rich and new results. It is able to reproduce the structural properties of homogeneous plots and spatial migrations of forest communities. Therefore, it is an efficient tool for understanding the long term dynamics of tropical rain forests from a theoretical viewpoint but also for assessing rain forest management scenarios.

Acknowledgements

References

Appanah, S., Weinland, G., Bossel, H., Krieger, H., 1991. Are tropical forests non-renewable? An enquiry through modelling. J. Trop. Forest Sci. 2, 331–348.

Ashton, P.S., 1978. Crown characteristics of tropical trees. In: Tomlinson, P.B., Zimmermann, M.H. (Eds.), Tropical Trees as Living Systems. Cambridge University Press, pp. 591–615.

Augspurger, C.K., 1984. Seedling survival of tropical tree species: interactions of dispersal distance, light-gaps, and pathogens. Ecology 65, 1705–1712.

Bossel, H., Krieger, H., 1994. Simulation of multi-species tropical forest dynamics using a vertically and horizontally structured model. Forest Ecol. Manage. 69, 123–144.

Botkin, D.B., Janak, J.F., Wallis, J.R., 1972. Some ecological consequences of a computer model of forest growth. J. Ecol. 60, 849–872.

Brokaw, N.V.L., 1982. The definition of treefall gap and its effect on measures of forest dynamics. Biotropica 14, 158–160.

Brokaw, N.V.L., 1984. Treefalls: frequency, timing, and consequences. In: Leigh, E.G., Rand, A.S., Windsor, D.M. (Eds.), The Ecology of a Tropical Forest: Seasonal Rhythms and Long Term Changes. Oxford University Press, pp. 101–108.

Bush, M.B., 1994. Amazonian speciation: a necessarily complex model. J. Bio-geog. 21, 5–17.

Canham, C.D., Denslow, J.S., Platt, W.J., Runckle, J.R., Spies, T.A., White, P.S., 1990. Light regimes beneath closed canopies and tree-fall gaps in temperate and tropical forests. Can. J. Forest Res. 20, 620–631.

Chandrashekara, U.M., Ramakrishnan, P.S., 1994. Vegetation and gap dynamics of a tropical wet evergreen forest in the western Ghats of Kerala, India. J. Trop. Ecol. 10, 337–354.

Charles-Dominique, P., Atramentowicz, M., Charles-Dominique, M., Gérard, H., Hladik, A., Hladik, C.M., Prévost, M.F., 1981. Les mammifères frugivores arboricoles nocturnes d'une forêt guyanaise: inter-relations plantes-animaux. Rev. Ecol. (Terre & Vie) 35, 341–434.

Charles-Dominique, P., Blanc, P., Larpin, D., Ledru, M.-P., Riéra, B., Sarthou, C., Servant, M., Tardy, C., 1998. Forest perturbations and biodiversity during the last ten thousand years in French Guiana. Acta Oecol. 19, 295–302.

Condit, R., Hubbell, S.P., Foster, R.B., 1995a. Mortality rates of 205 Neotropical tree and shrub species and the impact of a severe drought. Ecol. Monogr. 65, 419–439.

Condit, R., 1995b. Research in large, long-term tropical forest plots. Trends Ecol. Evol. 10, 18–22.

Dalling, J.W., Hubbell, S.P., Silvera, K., 1998. Seed dispersal, seedling establishment and gap partitioning among tropical pioneer trees. J. Ecol. 86, 674–689.

Deutschman, D.H., Levin, S.A., Devine, C., Buttel, L.A., 1997. Scaling from trees to forests: analysis of a complex simulation model. Science Online, available online at http://www.sciencemag.org.

Doligez, A., Joly, H.I., 1998. Fine-scale spatial genetic structure with nonuniform distribution of individuals. Genetics 148, 905–919.

Estrada, A., Fleming, T.H. (Eds.), 1986. Frugivorous and Seed Dispersal. Junk, Dordrecht.

Forget, P.-M., 1988. Dissémination et régénération naturelle de huit espèces d'arbres en forêt guyanaise, PhD report, Université Paris VI, 245 pp.

Gazel, M., 1983. Croissance des Arbres et Productivité des Peuplements en Forêt Dense Equatoriale de Guyane. Office National des Forêts, Direction Régionale de Guyane.

Gentry, A.H., 1989. Speciation in tropical forests. In: Holm-Nielsen, L.B., Nielsen, I.C., Balslev, H. (Eds.), Tropical Forests: Botanical Dynamics, Speciation and Diversity. Academic Press, pp. 113–124.

Gentry, A.H., Terborgh, J., 1990. Composition and dynamics of the Cocha Cashu 'mature' floodplain forest. In: Gentry, A. (Ed.), Four Neotropical Forests. Yale University Press, pp. 542–564.

Gourlet-Fleury, S., 1997. Modélisation individuelle spatialement explicite de la dynamique d'un peuplement de forêt dense tropicale humide, PhD report, Université Claude Bernard Lyon I, 274 pp + ann.

Hallé, F., Oldeman, R.A.A., Tomlinson, P.B., 1978. Tropical Trees and Forests. An Architectural Analysis. Springer, Berlin.

Henwood, K., 1973. A structural model of forces in buttressed tropical rain-forest trees. Biotropica 5, 83–93.

Herwitz, S.R., Young, S.S., 1994. Mortality, recruitment, and growth rates of montane tropical rain forest canopy trees on mount Bellenden-Ker, Northeast Queensland, Australia. Biotropica 26, 350–361.

Howe, H.F., 1983. Annual variation in a Neotropical seed-dispersal system. In: Sutton, S.L., Whitmore, T.C., Chadwick, A.C. (Eds.), Tropical Rain Forest: Ecology and Management. Blackwell Scientific, pp. 211–227.

Hubbell, S.P., Foster, R.B., 1990. Structure, dynamics, and equilibrium status of old-growth forest on Barro Colorado Island. In: Gentry, A. (Ed.), Four Neotropical Forests. Yale University Press, pp. 522–541.

Hubbell, S.P., Foster, R.B., O'Brien, T.S., Harms, K.E., Condit, R., Wechsler, B., Wright, S.J., Loo de Lao, S., 1999. Light-gap disturbances and recruitment limitation and tree diversity in a Neotropical forest. Science 283, 554–557.

Hurtt, G.C., Pacala, S.W., 1995. The consequences of recruitment limitation: reconciling chance, history and competitive differences between plants. J. Theor. Biol. 176, 1–12.

Jeník, J., 1978. Roots and root systems in tropical trees: morphologic and ecologic aspects. In: Tomlinson, P.B., Zimmermann, M.H. (Eds.), Tropical Trees as Living Systems. Cambridge University Press, pp. 323–349.

Kira, T., 1978. Community architecture and organic matter dynamics in tropical lowland rain forests of Southeast Asia with special reference to Pasoh Forest, West Malaysia. In: Tomlinson, P.B., Zimmermann, M.H. (Eds.), Tropical Trees as Living Systems. Cambridge University Press, pp. 561–590.

Köhler, P., Huth, A., 1998. The effects of tree species grouping in tropical rain forest modelling-Simulations with the individual based model FORMIND. Ecol. Model. 109, 301–321.

Köhler, P., Huth, A., Ditzer, T., 1999. Concepts for the aggregation of tropical tree species into functional types and the application on Sabah's dipterocarp lowland rain forests. J. Trop. Ecol. (submitted).

Korning, J., Balslev, H., 1994. Growth rates and mortality patterns of tropical lowland tree species and the relation to forest structure in Amazonian Ecuador. J. Trop. Ecol. 10, 151–166.

Lang, G.E., Knight, D.H., 1983. Tree growth, mortality, recruitment, and canopy gap formation during a 10-year period in a tropical moist forest. Ecology 64, 1075–1080.

Lescure, J.-P., Puig, H., Riéra, B., Leclerc, D., Beekman, A., Beneteau, A., 1983. La phytomasse epigée d'une forêt dense en Guyane Française. Acta Ecol. 4, 237–251.

Lieberman, D., Lieberman, M., Peralta, M., Hartshorn, G.S., 1985a. Mortality patterns and stand turnover rates in wet tropical forest in Costa Rica. J. Ecol. 73, 915–924.

Lieberman, D., Lieberman, M., Hartshorn, G.S., Peralta, M., 1985b. Growth rates and age-size relationships of tropical wet forest trees in Costa-Rica. J. Trop. Ecol. 1, 97–109.

Lieberman, D., Hartshorn, G.S., Lieberman, M., Peralta, M., 1990. Forest dynamics at La Selva biological station, 1969–1985. In: Gentry, A. (Ed.), Four Neotropical Forests. Yale University Press, pp. 509–521.

Lischke, H., Löffler, T.J., Fischlin, A., 1996. Aggregation of individual trees and patches in forest succession models. preprint ETHZ 28, 1996.

Liu, J., Ashton, P.S., 1998. FORMOSAIC: an individual-based spatially explicit model for simulating forest dynamics in landscape mosaics. Ecol. Model. 106, 177–200.

Manokaran, N., Kochummen, K.M., 1987. Recruitment, growth and mortality of tree species in a lowland Dipterocarp forest in peninsular Malaysia. J. Trop. Ecol. 3, 315–330.

van der Meer, P.J., Bongers, F., Chatrou, L., Riéra, B., 1994. Defining canopy gaps in a tropical rain forest: effects on gap size and turnover time. Acta Ecol. 15, 701–714.

Moravie, M.-A., Pascal, J.-P., Auger, P., 1997. Investigating canopy regeneration process through spatial individual-based models: application to a wet evergreen forest. Ecol. Model. 104, 241–260.

Newbery, D.C., Campbell, E.J.F., Lee, Y.F., Risdale, C.E., Still, M.J., 1994. Primary lowland Dipterocarp forest at Danum Valley, Sabah, Malaysia: structure, relative abundance and family composition. Phil. Trans. Royal Soc. London B 335, 341–356.

Oldeman, R.A.A., 1990. Forests: Elements of Silvology. Springer, Berlin.

Pacala, S.W., Canharn, C.D., Saponara, J., Silander, J., Kobe, R., Ribbens, E., 1996. Forest models defined by field measurements: II. Estimation, error analysis and dynamics. Ecol. Monogr. 66, 1–44.

Pélissier, R., Riéra, B., 1993. Dix ans de dynamique d'une forêt dense humide de Guyane Française. Rev. Ecol. (Terre & Vie) 48, 21–33.

Phillips, O.L., Malhi, Y., Higuchi, N., Laurance, W.F., Núñez, P.V., Vásquez, R.M., Laurance, S.G., Ferreira, L.V., Stern, M., Brown, S., Grace, J., 1998. Change in the carbon balance of tropical forests: evidence from long-term plots. Science 282, 439–442.

van der Pijl, L., 1982. The Principles of Dispersal in Higher Plants, 3rd. Springer, Berlin.

Prentice, I.C., Leemans, R., 1990. Pattern and process and the dynamics of forest structure: a simulation approach. J. Ecol. 78, 340–355.

Putz, F.E., Milton, K. Jr., 1982. Tree mortality rates on Barro Colorado Island. In: Leigh, E.G. Jr., Rand, A.S., Windsor, D.M. (Eds.), The Ecology of a Tropical Forest: Seasonal Rhythms and Long Term Changes. Smithsonian Institution Press, Washington, pp. 95–100.

Raich, J.W., Gong, W.K., 1990. Effects of canopy openings on tree seed germination in a Malaysian Dipterocarp forest. J. Trop. Ecol. 6, 203–217.

Rankin-de-Merona, J.M., Hutchings, R.W., Lovejoy, T.E., 1990. Tree mortality and recruitment over a five-year period in undisturbed upland rainforest of the Central Amazon. In: Gentry, A.H. (Ed.), Four Neotropical Forests. Yale University Press, pp. 573–584.

Ribbens, E., Silander, J.A. Jr., Pacala, S.W., 1994. Seedling recruitment in forests: calibrating models to predict patterns of tree seedling dispersion. Ecology 75, 1794–1806.

Richards, P.W., 1996. The Tropical Rain Forest, 2nd edn., Cambridge University Press, 575 pp.

Riéra, B., 1982. Observations sur les chablis. Piste de Saint-Elie, Guyane. Bulletin de Liaison de Groupe de Travail sur l'Ecosystème Forestier Guyanais, ORSTOM. Cayenne 6, 165–183.

Riéra, B., Alexandre, D.Y., 1988. Surface des chablis et temps de renouvellement en forêt dense tropicale. Acta Ecol. 9, 211–220.

Riéra, B., 1995. Rôle des perturbations actuelles et passées dans la dynamique et la musique forestière. Revue d'Ecologie (Terre e Vie) 9, 209–222.

Rollet, B., 1973. L'Architecture des Forêts Denses Humides Sempervirentes de Plaine. Centre Technique Forestier Tropical, Nogent-sur-Marne, France.

van Roosmalen, M.G.M., 1985. Fruits of the Guiana Flora. Institute of Systematics and Botany, Utrecht.

Runkle, J.R., 1981. Gap regeneration in some old-growth forests of the Eastern United States. Ecology 62, 1041–1051.

Sabatier, D., 1985. Saisonnalité et déterminisme du pic de fructification de forêt Guyanaise. Rev. Ecol. (Terre & Vie) 40, 289–320.

Schenk, H.J., 1996. Modelling the effects of temperature on growth and persistence of tree species: a critical review of tree population models. Ecol. Model. 92, 1–32.

Schupp, E.W., 1988. Factors affecting post-dispersal and seed survival in a tropical forest. Ecologia 76, 525–530.

Schwartz, D., de Foresta, H., Mariotti, A., Balesdent, J., Massimba, J.P., Girardin, C., 1996. Present dynamics of the savanna-forest boundary in the Congolese Mayombe: a pedological, botanical and isotopic (^{13}C and ^{14}C) study. Oecologia 106, 516–524.

Servant, M., Maley, J., Turcq, B., Absy, M.L., Brenac, P., Fournier, M., Ledru, M.P., 1993. Tropical rain forest changes during the late quaternary in African and South American lowlands. Global Planet. Change 7, 25–40.

Shugart, H.H., Hopkins, M.S., Burgess, I.P., Mortlock, A.T., 1980. The development of a succession model for subtropical rain forest and its application to assess the effects of timber harvest at Wiangaree State Forest, New South Wales. J. Environ. Manage. 11, 243–265.

Shugart, H.H., 1984. A Theory of Forest Dynamics. Springer, New-York.

Slatkin, M., Anderson, D.J., 1984. A model of competition for space. Ecology 65, 1840–1845.

Swaine, M.D., Hall, T.B., Alexander, I.J., 1987a. Tree population dynamics at Kade, Ghana. J. Trop. Ecol. 3, 331–345.

Swaine, M.D., Lieberman, D., Putz, F.E., 1987b. The dynamics of tree populations in tropical forest: a review. J. Trop. Ecol. 3, 359–366.

Swaine, M.D., Whitmore, T.C., 1988. On the definition of ecological species groups in tropical forests. Vegetation 75, 81–86.

Umeki, K., 1995. Modeling the relationship between the asymmetry in crown display and local environment. Ecol. Model. 82, 11–20.

Vanclay, J.K., 1995. Growth models for tropical forests: a synthesis of models and methods. Forest Sci. 41, 7–42.

Vanclay, J.K., Skovsgaard, J.P., 1997. Evaluating forest growth models. Ecol. Model. 98, 1–12.

Vasquez-Yanes, C., Guevara-Sada, S., 1985. Caracterizacion de los grupos ecologicos de arboles de la selva humeda. Regeneracion de Selvas II, Compania Editorial Continental, Mexico, pp. 67–78.

Whitmore, T.C., 1998. An Introduction to Tropical Rain Forests, 2nd edn, Oxford University, Oxford, 282 pp.

Young, T.P., Perkocha, V., 1994. Treefalls, crown asymmetry and buttresses. J. Ecol. 82, 319–324.